

Corelli: Efficient single crystal diffraction with elastic discrimination

STEPHAN ROSENKRANZ* and RAYMOND OSBORN

Materials Science Division, Argonne National Laboratory, Argonne, IL 60439, USA

*Corresponding author. E-mail: srosenkranz@anl.gov

Abstract. Single crystal diffuse scattering provides one of the most powerful probes of short-range correlations on the 1–100 nm scale, which often are responsible for the extreme field response of many emerging phenomena of great interest. Accurate modeling of such complex disorder from diffuse scattering data however puts stringent experimental demands, requiring measurements over large volumes of reciprocal space with sufficient momentum and energy resolution. Here, we discuss the potential of the cross-correlation technique for efficient measurement of single crystal diffuse scattering with energy discrimination, as will be implemented in a novel instrument, Corelli. Utilizing full experiment simulations, we show that this technique readily leads up to a fifty-fold gain in efficiency, as compared to traditional methods, for measuring single crystal diffuse scattering over volumes of reciprocal space with elastic discrimination.

Keywords. Neutron diffraction; diffuse scattering; elastic discrimination.

PACS Nos 61.05.F; 61.50.-f; 61.43.-j; 61.44.n

1. Introduction

Many phenomena of current interest are controlled by the introduction of complex disorder in crystalline solids, characterized by short-range correlations that extend from 1 to 100 nm [1]. Examples where disorder, and the associated nanoscale self-organization, results from the competition between ground states with incompatible order include colossal magnetoresistance, relaxor ferroelectricity, negative thermal expansion, quantum spin liquids, and high temperature superconductivity. Obtaining a detailed understanding of such complex disorder is therefore of great importance in condensed matter, with potential for impact on many other fields [2].

Single crystal diffuse scattering has the potential to provide the most powerful probe of complex disorder as it not only measures the existence and morphology of local distortions, but also directly probes defect–defect correlations, i.e., the tendency for defects to cluster into nanoscale ordered structures ([3–6] and references therein). However, obtaining a realistic physical understanding of how a material is locally organized puts stringent experimental demands, usually requiring measurements over large volumes of reciprocal space with sufficient momentum and energy

resolution to distinguish the various scattering constituents. Current instrumentation is either suited to measurements over large momentum range without energy discrimination, such as time-of-flight white-beam Laue instruments, or provides sufficient energy discrimination but only over a limited range of momentum space. In order to overcome these limitations we propose to implement the old idea of using cross-correlation to obtain energy discrimination in a dedicated diffuse scattering instrument at a pulsed neutron source to provide efficient measurements of diffuse scattering with both coverage of large volumes of momentum space and sufficiently high energy resolution.

2. Cross-correlation

The goal of the cross-correlation technique is to maximize the utilization of the available neutron flux by exploiting modulation of the incident neutron beam. The use of this technique for neutron scattering was intensively investigated in the late sixties and early seventies, mainly relating to steady state sources and beam modulations obtained using mechanical choppers [7–10], but it was also adapted for periodically modulated sources, such as long pulse reactors available at the time [11,12]. This generalization of the technique can be applied equally well to the new generation of short-pulsed spallation neutron sources and the proof of the principle was later carried out in the mid-eighties at IPNS [13]. The possibilities and benefits of utilizing modulation of the polarization was also discussed earlier in [14,15] and used in a few experiments.

The cross-correlation technique differs from traditional time-of-flight spectrometers, which only use a very narrow band of fixed incident or final energy, in that the incident neutron pulse is modulated in time in a pseudorandom fashion. The signal recorded at the detector is then no longer directly proportional to the sample scattering function $S(Q, \omega)$, but for a fixed total time-of-flight is the sum over all energy transfers ω for which the neutron was allowed to pass the chopper, as schematically illustrated in figure 1. The full $S(Q, \omega)$ can then however be reconstructed by forming the cross-correlation of the measured data with the modulation sequence, allowing utilization of up to 50% of the incident wavelength spectrum compared to typically 1–5% of a traditional time-of-flight spectrometer. But because of the cross-correlation, the statistical errors of the derived scattering function are now correlated among different channels leading to poor statistics for weak signals, which has led to the demise of the correlation technique for general spectroscopy. At a pulsed source however, the cross-correlation is performed only across the incident time-of-flight, which means that errors in the reconstructed $S(Q(\omega), \omega)$ are only correlated along the energy transfer ω , but for a fixed energy transfer ω are independent of the momentum transfer \mathbf{Q} . A strong signal that is localized in momentum space, such as a Bragg peak, therefore only adversely affects the statistics in a small volume around the Bragg peak position. The correlation method therefore has a tremendous potential for providing efficient measurements of single crystal diffuse scattering over large volumes of reciprocal space with elastic discrimination, where we wish to discriminate inelastic scattering, e.g. phonon scattering, that is in the same order of magnitude or weaker than the elastic signal.

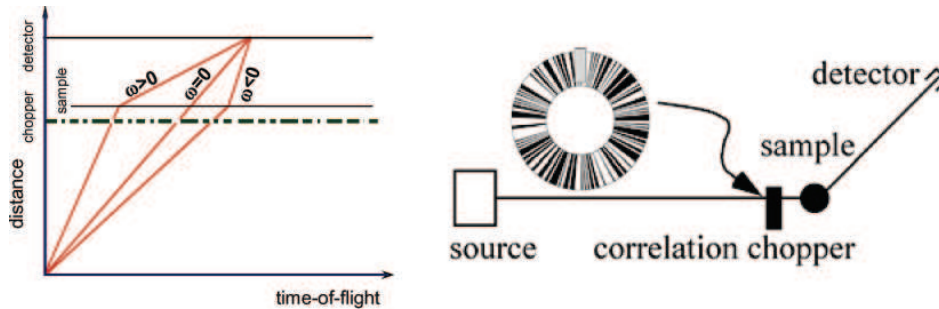


Figure 1. Illustration of the intensity measured with the cross-correlation technique at fixed total time-of-flight (left) and schematic of the simplified instrument used for the simulations (right).

3. Full experiment simulations and discussion

In order to prove the feasibility and obtain a realistic estimate of the gain in efficiency achievable by utilizing cross-correlation to obtain energy discrimination for single crystal diffuse scattering, we performed full experiment simulations utilizing McStas [16] with specialized routines for chopper and sample components. For this purpose we use a simplified instrument, schematically shown in figure 1, that incorporates only the source, a pseudorandom chopper, a sample, and a single point detector at a fixed scattering angle. For the simulations we utilized parameters relevant to Corelli, the dedicated single crystal diffuse scattering instrument under development at SNS, i.e., facing the high-resolution water moderator [17], a disk chopper with a radius of 35 cm running at 350 Hz and a 255 element pseudorandom sequence 19 m from the moderator, the sample at 1 m from the chopper, and a 1 cm \times 1 cm detector 2.5 m from the sample. We first simulate a powder sample using a harmonic oscillator model with $\hbar\omega_0 = 2$ meV, including excitations up to the fifth harmonic.

Figure 2 shows the resulting intensity for a single point detector as a function of total time-of-flight and phase-offset of the pseudorandom sequence with respect to the source pulse. Since the cross-correlation is performed over the phase-offset, it is necessary to sample the total time-of-flight spectrum for all possible offsets with the same probability, which is easily and almost instantaneously obtained by running the chopper asynchronously with the source. The right panel of figure 2 shows the cross-correlated data, which clearly demonstrates the reconstruction of the scattering function with the elastic scattering clearly separated from the inelastic excitations. This is seen more clearly in figure 3, which compares a single spectrum with constant incident energy extracted from the cross-correlated data from the enlarged region shown in figure 2, with the spectrum obtained using a conventional, single-aperture chopper with a corresponding fixed incident energy. The conventional chopper is clearly able to resolve all excitations up to and including the fifth harmonic, whereas the correlation chopper surprisingly can still resolve up to the fourth harmonic on the neutron energy loss side, which is more than an order of magnitude weaker than the strongest signal, and the third harmonic on

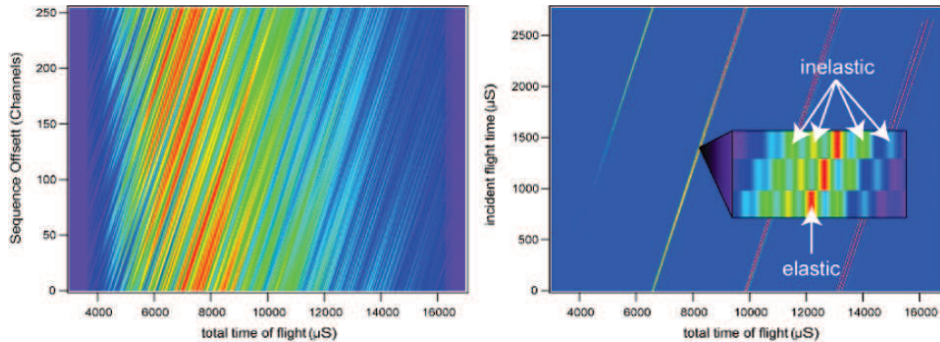


Figure 2. Intensity measured by the detector as a function of total time-of-flight and correlation sequence phase-offset and the corresponding cross-correlated data obtained for the full experiment simulations using a harmonic oscillator sample.

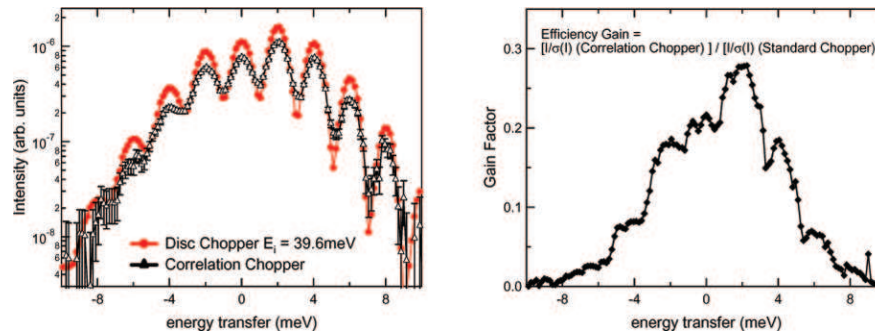


Figure 3. Comparison of a single spectrum with fixed incident energy extracted from the cross-correlated data with the spectrum measured with a traditional single-aperture chopper (left) and corresponding gain in efficiency of the cross-correlation (right).

the energy loss side is just still visible. For this comparison of a single spectrum, the cross-correlation is always less efficient than the traditional chopper as seen from the gain factor shown in figure 2, which is always < 1 . The cross-correlation technique however simultaneously measures a wide band of incident energies, i.e., provides hundreds of spectra corresponding to varying incident energies at once. This, in turn, means that the elastic intensity $S(Q, \omega = 0)$, which we are interested in, is obtained over a large range of momentum transfer at once, resulting in an actual total gain in efficiency of the cross-correlation method of the order of 30–50 for measuring the elastic scattering signal with sufficient energy discrimination.

We further illustrate this gain in efficiency obtained from the simultaneous coverage of a large range of momentum transfer of even a single detector pixel by extracting the elastic intensity from the simulated data. For this purpose, we simulate a perfect incoherent scatterer, for which the total scattering $S(Q)$ is constant as a function of momentum transfer, whereas the elastic intensity decays

Single crystal diffraction with elastic discrimination

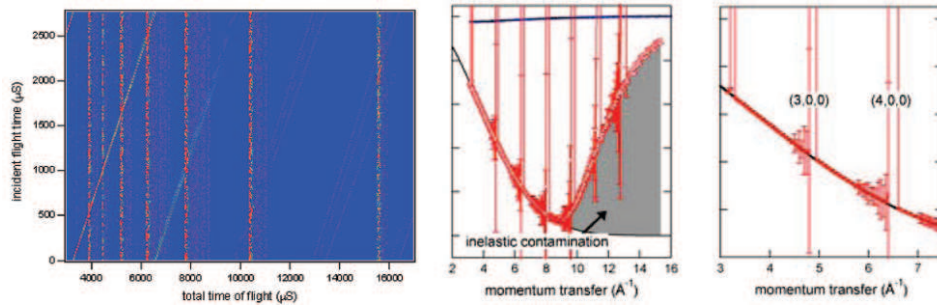


Figure 4. Full experiment simulation using a perfect coherent scatterer and including Bragg peaks. The middle panel shows the elastic scattering extracted from the cross-correlated data in red and the total scattering $S(Q)$ in blue. The right panel shows an enlarged region from the middle panel around the (3,0,0) and (4,0,0) Bragg peaks.

according to the Debye–Waller factor $S(Q, \omega = 0) \sim \exp(-2W(Q))$ with the remaining intensity distributed over the inelastic channels. Here, we use a simplified scattering function with all the inelastic scattering in a single excitation at ± 5 meV. We furthermore include a set of Bragg peaks, simulating a cubic sample with lattice constant $a = 3.875$ Å, aligned such that the $(h, 0, 0)$ peaks are in Bragg condition at a scattering angle of 90° , with the intensity of the Bragg peaks chosen to be three orders of magnitude stronger than the incoherent scattering at $Q = (4, 0, 0)$. The cross-correlated data obtained from these simulations shows streaks along the cross-correlation direction at the Bragg peak positions (figure 4). This is because the color scale of this figure is chosen such that the incoherent scattering remains visible and thus the Bragg peaks are strongly oversaturated. The streaks then appear because of the poor statistics of the cross-correlation in the presence of the very strong Bragg peaks. The true signal along these streaks would be zero, except for the incoherent scattering at 0 and ± 5 meV, but in the cross-correlation it is reconstructed as the difference of two large numbers, both in the order of the Bragg peak intensity, whose fluctuations are still stronger than the incoherent signal, giving rise to the streaks. The Bragg peaks however extend only over a very small range and therefore only affect a limited range of the data. This is clearly seen in the middle and right panels of figure 4, which show the elastic intensity $S(Q, \omega = 0)$ extracted from the cross-correlated data.

We first note, that the cross-correlation successfully provides the correct elastic intensity over a large range of momentum transfer as the extracted $S(Q, \omega = 0)$, represented by the red circles is identical to the theoretical intensity, shown as a black line, up to $Q \sim 9$ Å⁻¹ for a single point detector at a scattering angle of 90° . This elastic intensity is very different from the total scattering $S(Q)$, shown in blue, which for this sample is constant and is the quantity measured with a standard, energy integrating diffractometer. At higher momentum transfer, the elastic intensity extracted from the cross-correlated data starts to deviate from the Debye–Waller curve, approaching the total intensity $S(Q)$. This is because the energy resolution decreases with decreasing total time-of-flight and hence increasing momentum transfer. Upon increasing Q the energy discrimination therefore becomes

increasingly less effective and inelastic contamination finally leads to the deviation from the pure elastic signal towards the fully energy integrated $S(Q)$.

Close to the Bragg peak positions, the statistics of the elastic intensity extracted from the cross-correlated data becomes very poor. This is due to Bragg peak intensity leaking into the inelastic channels around the Bragg peak position due to finite energy resolution and sample mosaic. The usable range of momentum transfer over which the elastic intensity can be measured at once with the correlation method is however still considerably large even for this worst-case detector position exposed to a series of Bragg peaks. For comparison, a traditional single-aperture chopper instrument would only measure a single Q -point. We further note that the elastic intensity can be extracted without noticeable decrease in statistics even when it is less than 20% of the total $S(Q)$, which for the example used here is the case for $Q > 6 \text{ \AA}^{-1}$. As is seen from the right panel of figure 4, the extracted elastic intensity shows appreciable statistical errors only when it becomes contaminated from nearby Bragg peaks.

Last but not the least, we point out that the examples shown here represent worst-case detector positions, which actually contain Bragg peaks. The poor statistics of the elastic signal, because of nearby Bragg peaks, is by far the biggest concern for the efficiency of the cross-correlation for obtaining energy discrimination in diffuse scattering. In the absence of a Bragg peak, the intensity of the elastic signal, even for weak diffuse scattering, is usually in the order of the thermal diffuse scattering and therefore not small compared to the average signal over the whole energy spectrum, over which the cross-correlation is performed. And as we demonstrated above, the statistics of the elastic signal is not strongly degraded even when it only makes up $\sim 10\%$ of the total scattering. For single crystals the cross-correlation will provide poor statistics only over a very limited range of momentum transfer surrounding the Bragg peaks, the extent of which depends on beam divergences, sample size, mosaic and $\Delta d/d$. For the very large volume of reciprocal space not affected by this, our simulations prove that the cross-correlation at pulsed neutron sources provides a very efficient method to obtain energy discrimination in single crystal diffuse scattering.

Acknowledgement

This work is supported by US Department of Energy, Basic Energy Sciences, Department of Materials Science under contract DE-AC02-06CH11357.

References

- [1] A Moreo, S Yunoki and E Dagotto, *Science* **283**, 2034 (1999)
- [2] G Aeppli and G Chandra, *Science* **275**, 177 (1997)
- [3] T R Wellbery and B D Butler, *Chem. Rev.* **95**, 2369 (1995)
- [4] F Frey, *European J. Mineral.* **9**, 693 (1997)
- [5] V M Nielsd and D A Keen, *Diffuse neutron scattering from crystalline materials* (Clarendon Press, Oxford, 2001)
- [6] S Rosenkranz and R Osborn, *Neutron News* **15**, 21 (2004)

Single crystal diffraction with elastic discrimination

- [7] L Pal, N Kroó, P Pellionisz, F Szlavik and I Vizi, in *Neutron inelastic scattering* (I.A.E.A., Vienna, 1968) p. 407
- [8] K Sköld, *Nucl. Instrum. Methods* **63**, 114 (1968)
- [9] R von Jan and R Scherm, *Nucl. Instrum. Methods* **80**, 69 (1970)
- [10] D L Price and K Sköld, *Nucl. Instrum. Methods* **82**, 208 (1970)
- [11] W Matthes, in *Neutron inelastic scattering* (I.A.E.A., Vienna, 1968) p. 773
- [12] N Kroó, P Pellionisz, I Vizi, G Zsigmond and G Zhukov, in *Neutron inelastic scattering* (I.A.E.A., Vienna, 1968) p. 763
- [13] R K Crawford, J R Haumann, G E Ostrowski, D L Price and K Sköld, in *International Conference on Advanced Neutron Sources* (Argonne National Laboratory, Argonne, USA, 1986)
- [14] F Mezei and P Pellionisz, *Nucl. Instrum. Methods* **99**, 613 (1972)
- [15] R Cywinski and W G Williams, Rutherford Appleton Laboratory Report, RAL-84-062 (1984)
- [16] K Nielsen and K Lefmann, *Physica* **B283**, 426 (2000)
- [17] E B Iverson, P D Ferguson, F X Gallmeier and I I Popova (Spallation Neutron Source, 2002)